

QUANTITATIVE ANALYSIS OF PORE-PARTICLE-CORRELATIONS IN METALLIC FOAMS

A. Haibel¹, A. Bütow², A. Rack¹, and J. Banhart^{1,2}

¹Hahn-Meitner-Institute Berlin, ²Technical University, Germany

Abstract: Metallic foam characterization and development is of high interest in the material science. This paper presents a quantitative analysis of the pore-particle correlations in metallic foams based on tomographic experiments. The investigated materials consist of aluminium alloys with titanium hydride powder acting as blowing agent. In two sample series silicon carbide particles were additionally added as foam stabilizers. For the first time three dimensional the rearrangement of these SiC particles in the liquid metallic foam could be shown by means of synchrotron tomography. The quantitative analysis was performed by a special dilatation algorithm. In addition the correlation between particle sizes and pre-heat treatment of the blowing agent TiH₂ and the pore structure is presented.

Introduction: Metallic foams are highly porous materials with interesting properties. They distinguish themselves from other materials by low density, high specific stiffness, and high energy absorption capability [1,2]. Therefore they become more and more popular for industrial applications. In order to produce metallic foams with reproducible macroscopic properties, the precise knowledge of their microscopic structure is needed.

Our research topics aim at the understanding of the physical processes during foaming and at the optimisation of production by varying the manufacturing parameters. The chosen foam production route is to add some blowing agent, mostly titanium hydride, into a metallic precursor material [3]. To achieve a sufficient stability of the pores during the foaming process partially wetting, micrometer-sized, non-soluble particles can be admixed [4]. Due to their partial wetting property they accumulate on the pore surfaces and stabilize the cell walls. After heating up the precursor to above both the decomposition temperature of the blowing agent and the melting temperature of the metal, hydrogen is released in the melt and a porous structure is generated. The influence of both components, the blowing agent TiH₂ and the non-soluble particles SiC, on the foaming structure is investigated non-destructively by means of synchrotron tomography. By varying the blowing agent particle size the correlation between the different particle sizes and the pore size distributions was observed. Also the influence of a heating pretreatment of the blowing agent particles was studied. For the investigation of the rearrangement process of the non-soluble, partial wetting particles the three dimensional spatial distribution of silicon carbide particles in an unfoamed cast solid aluminium precursor, in the fully foamed liquid state of the material, and in the solidified final state of the foam was measured. Due to the tomographic investigations the rearrangement mechanism during the foaming process could be described.

Materials and Methods: The measurements were carried out using the BAMline (BAM, Federal Institute for Materials Research and Testing) at the Berlin electron storage ring company for synchrotron radiation (BESSY).

The highly intensive, monochromatic synchrotron radiation allows for a high spatial resolution (3.6 μm) and a very good signal-to-noise ratio. The X-ray energy range is adjustable between 6 and 60 keV.

To prepare the metallic foams with different blowing agent particle sizes TiH₂ was separated by sieving the particles with different mesh sizes. Using these TiH₂ particles two sample series were prepared, one using pre-heat treated blowing agent powder (particle sizes >20 μm, 40-20 μm, 40-80 μm), the other using untreated powder (40-20 μm, 40-80 μm and 80-160 μm). The treated TiH₂ powder causes a hydrogen release at higher temperatures (decomposition temperature T=520°C) than the untreated powder (T=400°C) [5]. The mixed metal and blowing agent powders were pressed and subsequent foamed in a specific heating form (sketched in Fig. 1). For all samples the foaming process was interrupted at the same foaming state 20 seconds after reaching the melting temperature. For the tomographic measurements rectangular samples with a profile of 4x4 mm were cut [6].

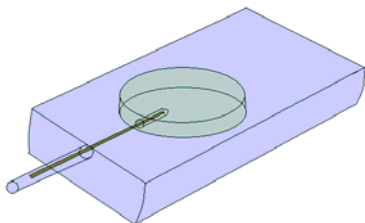


Fig.1: Heating form ensuring a reproducible, evenly distributed and fast heating-up of the precursor material. For measuring the exact sample temperature the thermocouple is placed directly inside the sample.

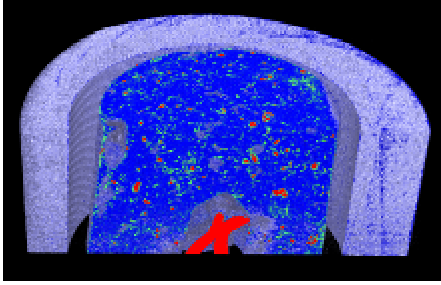


Fig. 3: Tomographic picture of the precursor material (AlSi10Mg, blue: aluminium alloy, cyan: SiC particle and red: TiH₂ particle) inside the glass tube. The thermocouple is placed at the bottom of the sample.

In a second experiment the rearrangement process of foam

stabilizing silicon carbide particles was investigated [7]. Two samples each with 10 vol.% partially wetting, micrometer-sized, non-soluble SiC particles (average size 70 μm and 13 μm) were studied in the solid precursor state, in the foamed liquid state and in the fully foamed solidified final state. For this in situ experiment a heating set up consisting of two heating lamps and a sample holder was employed for the foaming of the material during the tomographic measurements. As illustrated in Fig. 2 this sample holder involves a glass tube containing the sample and standing on refractory clay. Temperature control of the foam during the tomographic measurements is ensured by a rotatable thermocouple placed directly inside the sample. The foaming process took place at a temperature of $T=560^\circ\text{C}$ for the sample with 70 μm SiC particle size and at a temperature of $T= 570^\circ\text{C}$ for the sample with 13 μm SiC particle size. The measurement time was about 20 minutes and the energy was attuned to 30 keV.

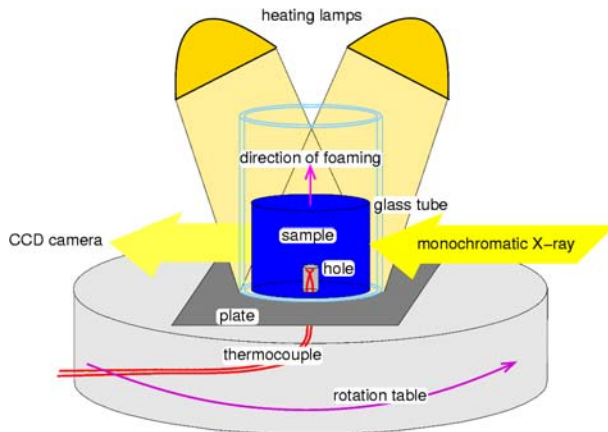


Fig. 2: Heating set up for tomography on liquid foams, consisting of two heating lamps and a sample holder made of a glass tube fixed on refractory clay. The glass tube stabilizes the foam in the liquid state. A thermocouple is located directly inside the sample.

Measurements: As an example for the tomographic results Fig. 3 shows a 3D image of the precursor alloy AlSi10Mg with 70 μm SiC particle size inside the glass tube. The SiC particles (cyan) and the blowing agent particles (red) are clearly distinguishable from the aluminium matrix (blue). Fig. 4 displays three tomographic 2D slices of the sample with 70 μm SiC particle size. The left picture shows the solid precursor state with some initial pores in the material. The centered picture shows a tomographic slice of the same sample in the liquid foamed state and the picture to the right displays the sample in the solidified foamed state.

The first visual result shows that in the unfoamed state the SiC particles are distributed rather homogeneously. In the liquid as well as in the solidified state a slight rearrangement process takes place.

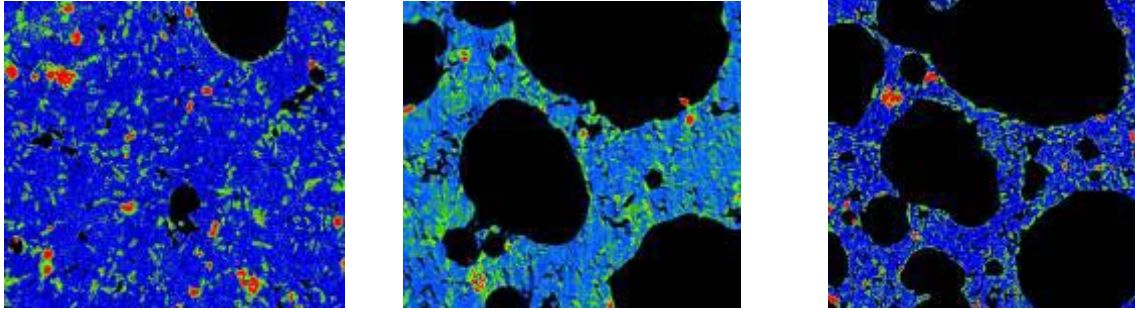


Fig. 4: AlSi10Mg (blue) with 70 μm sized SiC particles (cyan) and 0.5 vol.% TiH₂ particles (red). Side length: 3 mm. Left: Cast solid precursor with some initial pores. Center: Full foamed liquid state of the sample. Right: Solidified foamed state.

The tomographic pictures in Fig. 5 differ from those in Fig. 4 only by the silicon carbide particle size which is 13 μm . Here a correlation between pores and particle accumulation is obvious. The particles accumulate preferably on the initial pore surfaces already in the unfoamed solid state but most clearly in the liquid as well as in the solidified state. Furthermore the cell wall thickness is much smaller here than for the sample with 70 μm SiC particle size, i.e. the porosity is much higher.

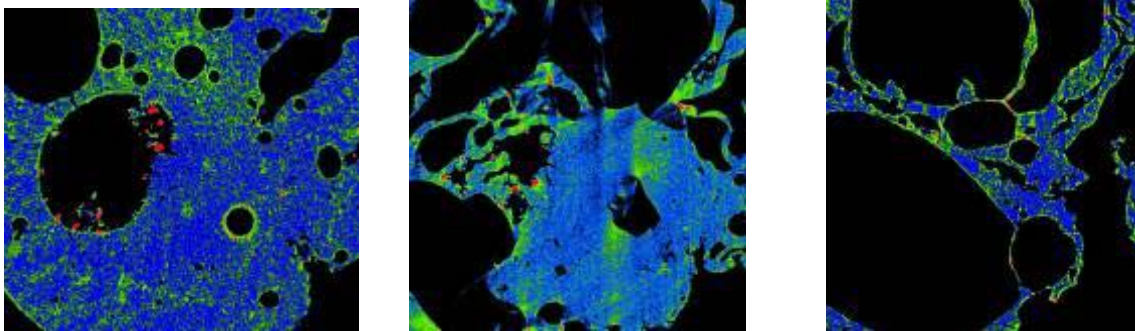
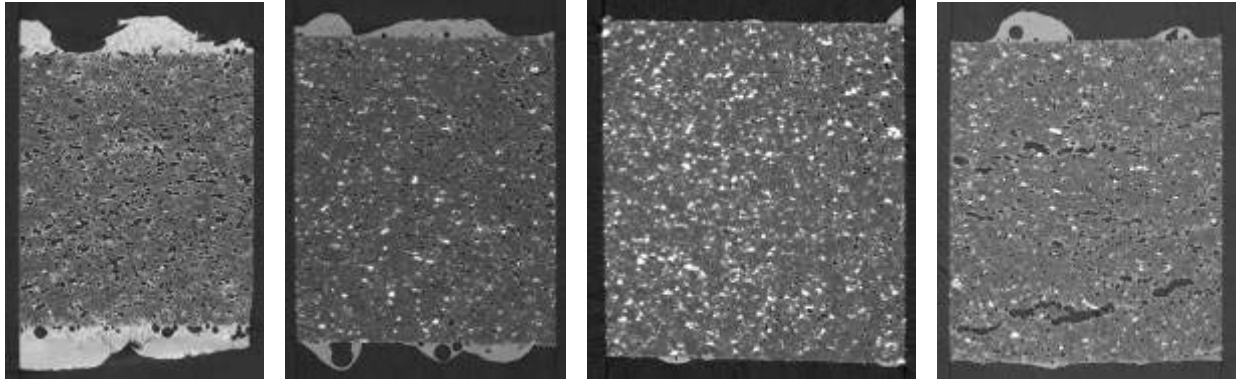


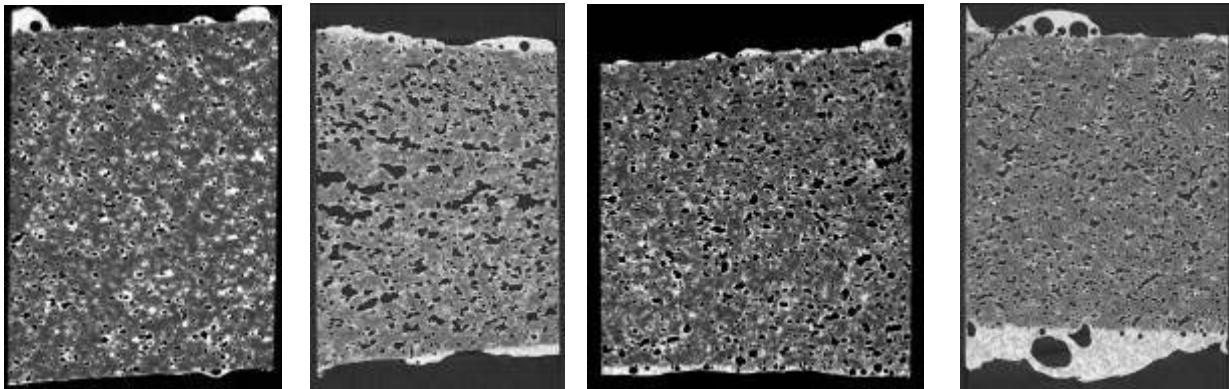
Fig. 5: AlSi10Mg (blue) with 13 μm sized SiC particles (cyan) and 0.5 vol.% TiH₂ particles (red). Side length: 3 mm. Left: Cast solid precursor with a lot of initial pores. Center: picture of the full foamed liquid state of the material. Right: The solidified foamed material.

The tomographic measurements of the aluminium alloy AlSiCu with different blowing agent particle sizes are displayed in Fig. 6. The first four pictures show the pore size distribution of the metallic foam produced with untreated TiH₂ whereas the second four pictures show the tomographic measurements of the material foamed with treated TiH₂. Both sample series are in the same early foaming state. As a first result we see the pores of the samples with treated TiH₂ are always larger than the pores foamed with untreated TiH₂. Furthermore the pore size distribution of the material with untreated blowing agent is mostly independent of the used TiH₂ particle size (except the sample with the unsieved blowing agent powder, where cracks vertical to the pressure direction occur). For the sample series with pre-heat treated blowing agent a maximum of the pore size at TiH₂ particles of 20-40 μm can be observed.

Also the blowing agent particle size seems to be smaller for treated than for untreated TiH₂. During the sieving of treated powder more smaller TiH₂ particles (<20 μm) were found, whereas untreated blowing agent powder contained more larger particles (80-160 μm). In all pictures a copper enriched phase appears at the sample surfaces (see Fig. 6).



Sample series of AlSiCu foamed with **untreated** blowing agent powder.



Sample series of AlSiCu foamed with **treated** blowing agent powder.

Fig. 6: Tomographic slices of the foamed aluminium alloy AlSiCu. The first four samples were foamed with untreated blowing agent powder, the second four with pre-heat treated powder. The variation parameter was the blowing agent particle size. The particle size ranges for sample series with **untreated** powder are 20-40 μm , 40-80 μm and 80-160 μm and the particle size ranges for sample series with **treated** TiH_2 are <20 μm , 20-40 μm and 40-80 μm . Due to the treatment the size distribution of the treated TiH_2 shifts to smaller particles. As a basis for comparison between the results of the samples with sieved blowing agents the samples with unsieved TiH_2 were additionally investigated.

Results and discussion: The first step towards a quantitative analysis of tomographic pictures is to plot a histogram. In a histogram all voxels of a 3D tomographic record are plotted sorted by their grey values, which corresponds to the absorption coefficients of the different components of the samples. As an example for the sample series with different blowing agent particle size distributions two histograms (left: unfoamed, right: foamed) of the aluminium alloy with treated, 40-80 μm sized TiH_2 are displayed in Fig. 7. The alloying of the components TiH_2 and copper during the foaming process can clearly be seen due to the decreasing of the high absorbing part in the histogram.

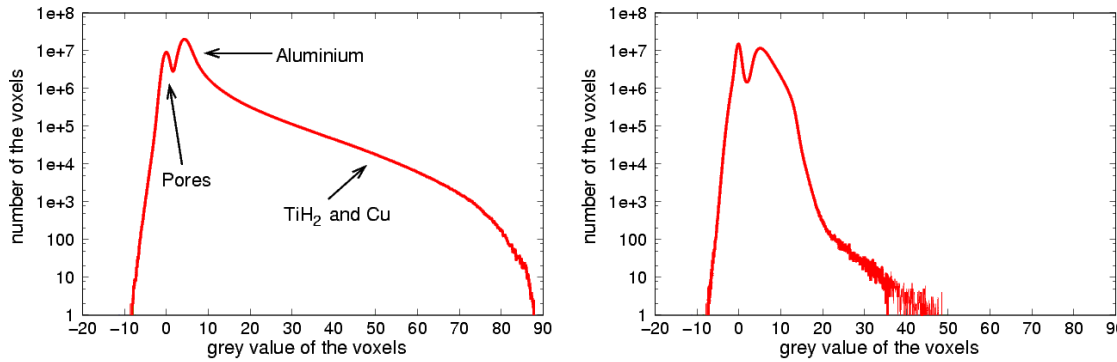


Fig. 7: Histograms of the tomographic records of the unfoamed as well as the foamed aluminium alloy AlSiCu with 40-80 μm sized treated TiH_2 . The first peak around zero can be dedicated to the pores. The second one is the aluminium peak. The right wide shoulder generated by the high absorbing components TiH_2 and copper in the unfoamed state disappears in the foamed state due to alloying of the single components with aluminium.

Fig. 8 presents a histogram of the aluminium alloy AlSi10Mg with admixed SiC particles inside a glass tube (see Fig. 3). The highest absorption value can be assigned to the thermocouple made of NiCr and Ni. The absorption values of the different sample components and of the glass tube are shown in the enlarged part of the histogram.

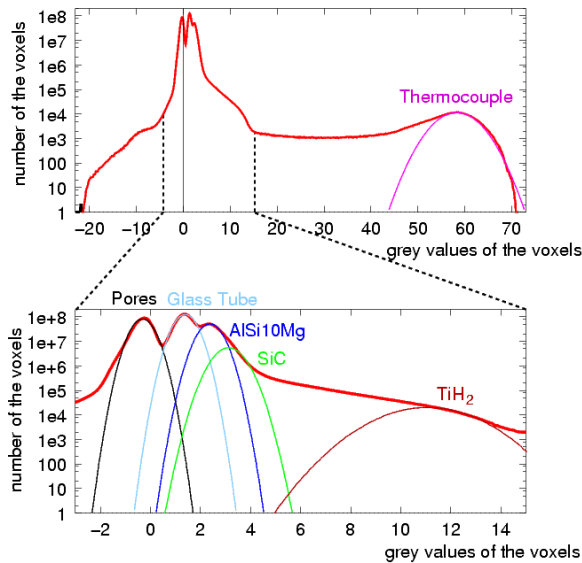


Fig. 8: Histogram of the aluminium alloy AlSi10Mg inside the glass tube as shown in Fig. 3. The thermocouple has the highest absorption value. In the close up view the absorption coefficients of the different sample components and of the glass tube are shown. The pores without absorption have grey values around zero and the glass tube has only a weak absorption. The aluminium alloy and the silicon carbide particles have nearly the same absorption coefficient, and the high absorbing shoulder can be assigned to the blowing agent TiH_2 .

By means of these histograms it is possible to separate the information of the tomographic data into Boolean 3D images of the found distinguishable components. Using a growth algorithm and by choosing the thresholds from the histogram all grey values belonging to one certain component are assigned in separate records as sketched in Fig. 9. The selected voxels of the record are assigned to have the value one, the other voxels zero. Such Boolean records are used for the quantitative 3D image analysis.

Thus, in order to quantify the spatial correlation between the pores in the aluminium alloy AlSi10Mg and the SiC particle positions, the pores identified in the binary 3D records were successively dilated step by step with a special growth algorithm [7]. After each of these dilatation steps those SiC particle voxels that became included in the increasing pore volume were counted, as sketched in Fig. 10.

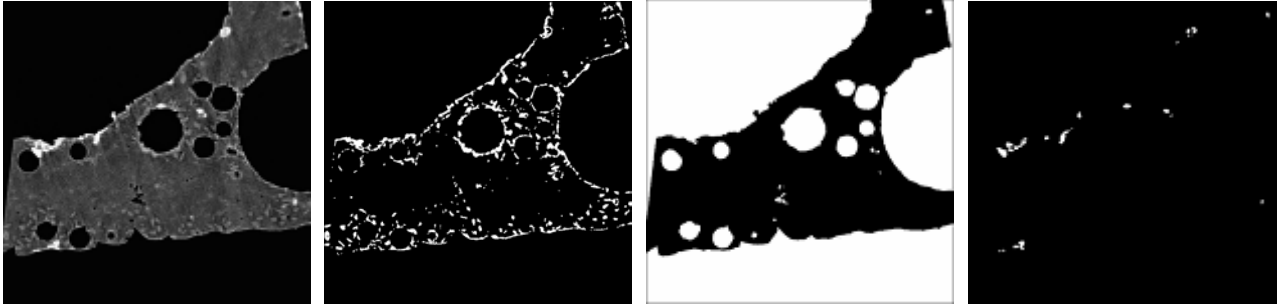


Fig. 9: Example for the separation process of the various components in a tomographic image into separate records. The first picture shows a 2D close-up of a tomographic image taken up from AlSi10Mg + 10 vol.% SiC particles (average size 70 μm) + 0.5 vol.% TiH₂. The next three pictures show the separated information on the silicon carbide (second image), the pores (third image), and the titanium hydride (last image) alone.

In the first image the initial situation is plotted. Both Boolean records, pores and SiC particles, lie on top of each other. The pore information is shown in white and the particle information in green. The second image shows the result of the dilatation algorithm after five steps. The pores are blown up a few voxel layers, then all SiC particles found in the dilated pore volume (red coloured) are counted. The third picture shows the tenth dilatation step. In the last picture the pore volume is increased up to 99% of the whole sample volume and the calculation algorithm terminates.

If the fraction of added particles decreases while dilating, a spatial correlation between pore and SiC particle position exists. If the number of added particles is almost constant in each dilatation step, the spatial arrangement of pores and particles is independent, no correlations exist.

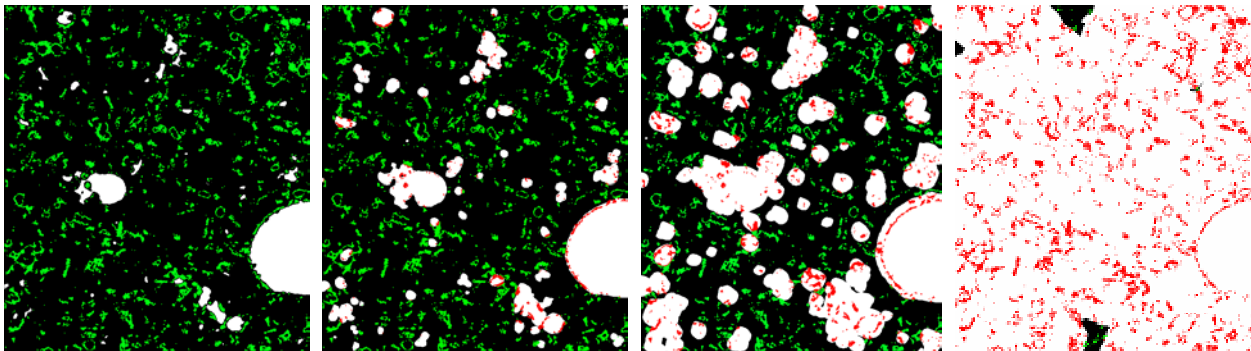


Fig. 10: As an illustration of the dilatation algorithm the two Boolean records (white: initial pores, green: SiC particles) of the unfoamed solid aluminium alloy AlSi10Mg are plotted. The initial pores accrue during the production process of the precursor material [3]. The first image shows the starting situation. In the following three pictures the initial pores were blown up and the SiC particle falling in the extended pore volume were counted (red coloured). In the second and the third image the situation after 5 and 10 dilatation steps is displayed. The fourth image shows the last dilatation step, where 99% of the sample volume is included.

In Fig. 11 the results of the correlation calculations are shown. In the diagrams the SiC particle density versus the dilatation step distance from the start pore surface is plotted. The first diagram presents the correlation results for the aluminium alloy AlSi10Mg containing 70 μm sized SiC particles. In the second diagram the results for the sample with 13 μm SiC particle size are plotted. The red curves represent the calculation for the unfoamed material. In both diagrams the values of these curves are almost constant. Only in the beginning the red curves decline due to the accumulation of SiC particles on the surfaces of the initial pores in the precursor material. After the heating up and the foaming process two measurements for each sample (70 μm and 13 μm SiC particle size) in the foamed liquid state were made. The green and the blue curves represent the correlation calculations between SiC particles and pores for this fully foamed, liquid state of the material. The green curves are

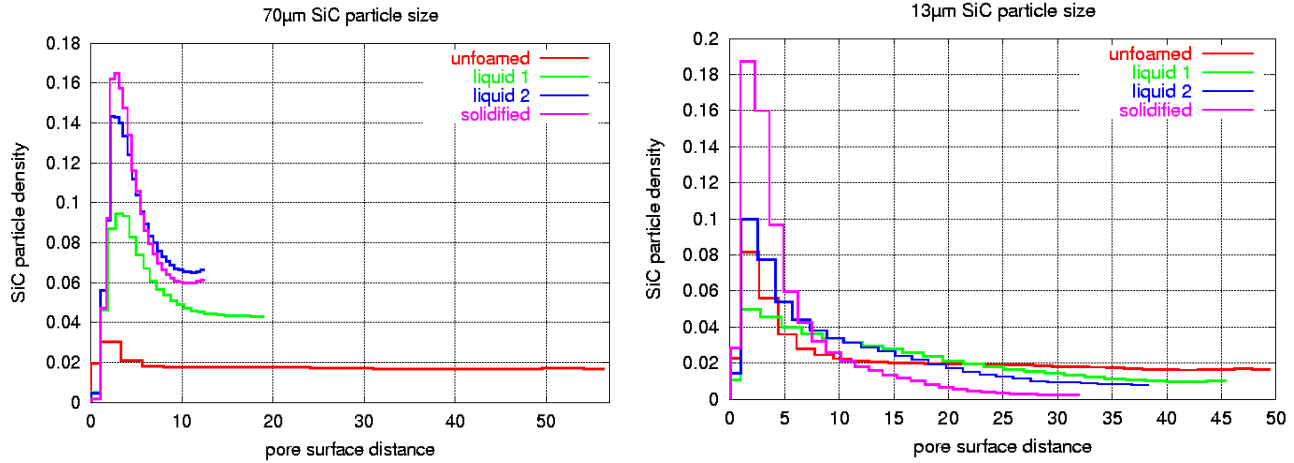


Fig. 11: Results of the dilatation algorithm for calculation the spatial correlation between pores and SiC particles in the unfoamed, the liquid foamed and the following solidified foamed state of the aluminium alloy AlSi10Mg mixed with 10% SiC particles. The left diagram show the results for a SiC particle size of 70 μm , the right diagram displays the results for the 13 μm particle sized SiC particle. All data are normalized of the area under the curves.

dedicated to the first liquid measurements, the blue curves to the seconds. All four curves show a marked decreasing behaviour, but the decreasing of the blue curves (second liquid measurement) is stronger and the dilatation step width away from the start pore surfaces is shorter. Generally, the slope of the four curves suggest an obvious rearrangement process of the SiC particles in the liquid state of the metallic foam, but much stronger for the samples with 13 μm particle size than for the samples with 70 μm sized particles. The stronger decreasing and the shorter pore surface distance of both blue curves seem to be due to the proceeding foaming process after the first measurement at the liquid state of the samples. Thus the accumulation process of the SiC particles continues and the pore size increase leads to an earlier termination of the dilatation algorithm since the investigated sample volume has decreased. The curves of the solidified foam (magenta coloured) show the strongest gradient, implying that the rearrangement process continues during the solidification.

The correlation between pores and blowing agent particles for the aluminium foam AlSiCu pictured in Fig. 6 was quantified by counting the pores with a labelling algorithm using the Boolean records and by specifying their volume. In Fig.12 the results are listed. Generally the porosity of samples foamed with untreated blowing agent is lower for all TiH₂ particle sizes as well as for unsieved particles (see Fig. 12 right, red boxes). The higher porosity of the samples prepared with treated blowing agents is due to the shift in the hydrogen release at higher temperatures (520°C) of this powder, which coincides much better with the melting temperature of the

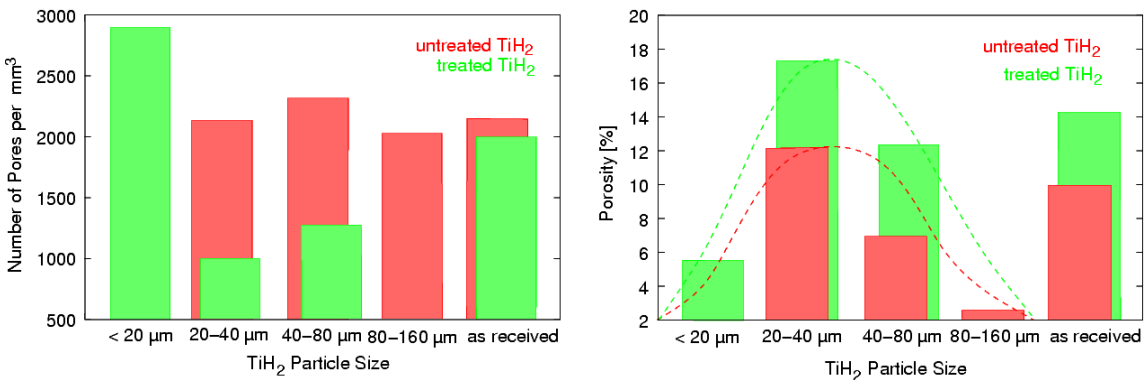


Fig. 12: Results of the correlation between pores and the blowing agent particle size. The green boxes represent the results for the treated blowing agent powder, the red boxes for the untreated powder. The left figure shows the number of pores versus the blowing agent particle size and in the right figure the porosity versus the blowing agent particle size is displayed. (The dashed lines are guides for the eyes.)

alloy (525°C). Therefore most hydrogen can be used for forming pores. The untreated powder, where the decomposition starts at $T=400^{\circ}\text{C}$, loses a part of the hydrogen before the alloy melts. Furthermore it seems that the blowing agent particle size for untreated powder has no influence on the pore size distribution (see Fig. 12 left, red boxes). However, for the samples foamed with treated blowing agent the pore size distribution seems to depend on the TiH_2 particle size (see Fig. 12, green boxes). All samples contain 1vol.% TiH_2 . Therefore the sample with the smallest particle sizes has the highest number of particles and after the foaming also the highest number of small pores. The particles with larger particle sizes (20-40 μm and 40-80 μm diameter), i.e. with a smaller number of particles produce a much lower number of pores but a higher porosity. The samples foamed with unsieved blowing agent powder show an average of the results produced with sieved blowing agents with respect to the number of pores as well as to the porosity. The highest porosity seems to occur with the particle size of 20-40 μm for the treated as well as for the untreated powder.

Conclusions: The results of tomographic investigations presented here have shown that synchrotron tomography is an appropriate measurement method for non-destructively analyzing the entire pore and particle formation of metallic foams and their correlation.

Two experiments developed for the investigation of pore-particle correlations in metallic foams were presented. For the first time tomographic measurements on liquid metallic foams were performed. The results of the measurements clarified the rearrangement process of SiC particles used as foam stabilizer during foaming. It could be shown that the accumulation process of the SiC particles on the pore surfaces takes place prevailing in the liquid state due to their partially wetting property. However, the process also continues during the solidification. It seems that due to the solidification front the particles were additionally pushed on the pore surfaces. Furthermore we could clearly verify that the rearranging for smaller SiC particles (13 μm) is much more significant than for the 70 μm sized SiC particles.

In a second experiment the influence of the blowing agent particle size and the blowing agent treatment on the foam structure was proven. We could show that the samples prepared with treated blowing agent powder have a higher porosity than the samples foamed with untreated blowing agent powder. In addition, for the samples prepared with untreated blowing agent the particle size has no influence on the number of pores whereas for the samples foamed with treated blowing agent the influence between blowing agent particle size and the number of pores is obvious. Finally, the highest porosity was reached for the blowing agent particles with 20-40 μm diameter.

We acknowledge H. Riesemeier, J. Goebbels, and G. Weidemann at the Federal Institute of Materials Research and Testing (BAM) for the experimental support.

References:

- [1] M. Ashby et al., *Metal foams: A Design Guide*, Butterworth-Heinemann (2000)
- [2] J. Banhart, N. Fleck, and A. Mortensen, eds., *Cellular Metals: Manufacture, Properties, Applications*, MetFoam 2003, MIT-Verlag Berlin 2003
- [3] J. Banhart, *Manufacture, characterisation and application of cellular metal foams*, progress in material science 46 (2001), 559-632
- [4] I. Jin, L. D. Kenny, and H. Sang, *Stabilized Metal Foam Body*, U.S. Patent 5 112 697, (1992)
- [5] B. Matijasevic, S. Fiechter, I. Zizak, O. Görke, N. Wanderka, P. Schubert-Bischoff, J. Banhart, *Decomposition behaviour of as-received and oxidized TiH_2 powder*, Powder Metallurgy World Congress, conference book (2004)
- [6] A. Bütow, diploma thesis, *Strukturuntersuchungen an Metallschäumen in verschiedenen Entwicklungsstadien*, Hahn-Meitner-Institut Berlin, SF3 (2004)
- [8] A. Haibel, J. Banhart, *Synchrotron-Tomography on Metallic Foams*, Proceedings of the International Symposium on Computed Tomography and Image Processing for Industrial Radiology (2003)
- [7] J. Ohser and F. Mücklich, *Statistical Analysis of Microstructures in Material Science*, John Wiley & Sons (2000)